Inorganic Chemistry

Communication

pubs.acs.org/IC

Mechanochemical Preparation of Nanocrystalline BaFCl Doped with Samarium in the 2+ Oxidation State

Xiang-lei Wang,[†] Zhi-qiang Liu,[†] Marion A. Stevens-Kalceff,[‡] and Hans Riesen*[,†]

[†]School of Physical, Environmental and Mathematical Sciences, The University of New South Wales, ADFA, Canberra, Australian Capital Territory 2600, Australia

[‡]School of Physics and Electron Microscope Unit, Mark Wainwright Analytical Centre, The University of New South Wales, Sydney, New South Wales 2052, Australia

Supporting Information

ABSTRACT: We report a facile mechanochemical preparation method for nanocrystalline BaFCl doped with samarium in the 2+ oxidation state by ball milling $BaCl_2$, BaF_2, and SmI_2 under a nitrogen atmosphere. The resulting phosphors were characterized by powder X-ray diffraction; electron microscopy, X-ray photoelectron spectroscopy; and photoluminescence, photoexcitation, cathodoluminescence, and diffuse reflectance spectroscopy. This is the first report of a direct preparation method of Sm^{2+} doped alkaline earth fluorohalides at room temperature and points to a significant potential for the preparation of a wide range of related X-ray storage phosphors containing rare earth ions in divalent and trivalent cationic states by mechanochemical methods.

The luminescence properties of inorganic materials activated by Sm ions, either in their divalent or trivalent oxidation states, have been widely investigated due to their potential applications as solid-state lasers, luminescence materials, and optical data storage media.[1−3] In particular, considerable attention has been directed to the Sm^{2+} doped alkaline earth fluorohalides MFX (M = Ca, Sr, or Ba; X = Cl, Br, or I) since the first observation of photon-gated spectral hole-burning was reported for BaFCl:Sm^{2+};[4] it is widely believed that Sm^{2+} may be the key to very high-density frequency domain optical data storage. The divalent state is, in general, obtained by the reduction of Sm^{3+} ions at elevated temperatures in a reducing atmosphere, e.g., flowing H_2 gas,[5] N_2−H_2 gas mixtures,[6] H_2−Ar gas mixtures,[7] or in air without a nominal reducing agent[2,8,9] and by exposure to ionizing radiation, including X-rays,[10] γ-irradiation,[11] β-irradiation,[12] and femtosecond laser light.[13] On the basis of the reduction of Sm^{3+} to Sm^{2+} upon exposure to ionizing radiation, we have shown that nanocrystalline BaFCl:Sm^{3+} can also serve as an efficient X-ray storage phosphor[14−17] with applications in medical imaging and dosimetry.

The reduction potential for $Sm^{3+} + e^- \rightarrow Sm^{2+}$ is −1.55 V and hence much lower than that of $Eu^{3+} + e \rightarrow Eu^{2+}$, which is −0.36 V.[18] Thus, Sm^{2+} is highly unstable in aqueous solutions, unlike Eu^{2+} which can be obtained by reduction of Eu^{3+} in water under N_2 by employing granular zinc. This was applied to prepare nanocrystalline BaFCl:Eu^{2+} by coprecipitation.[19]

Ball-milling has been used for grinding, mixing, and homogenizing nanomaterials.[20] We have recently reported the preparation of BaFCl:Sm^{3+} X-ray storage phosphor by ball milling.[21] In the present Communication, we report a mechanochemical method for preparing nanocrystalline BaFCl doped with Sm^{2+} by ball milling $BaCl_2$, BaF_2, and SmI_2 under a nitrogen atmosphere. This is the first report on a facile and direct preparation method for Sm^{2+} doped alkaline earth fluorohalides at room temperature, a significant outcome given the very high oxidation potential of Sm^{2+} (+1.55 V).

ACS reagent grade chemicals were used without further purification. Typically, the nanocrystalline BaFCl:Sm^{2+} was prepared by ball milling a mixture of 0.208 g $BaCl_2$ (1 mmol), 0.175 g BaF_2 (1 mmol), and 2 mg SmI_2 (∼0.25%; atom % relative to Ba) in a 10 mL zirconia jar with two 12 mm diameter zirconia balls on a Retsch Mixer Mill 200 at the frequency of 20 Hz for 120 min. Before ball milling, $BaCl_2$ and BaF_2 were ground separately and mixed together. The mixture was then dried under vacuum at 200 °C for 3 h. To avoid the oxidation of Sm^{2+} to Sm^{3+} ions in air, SmI_2 and the mixture of $BaCl_2$ and BaF_2 were added to the zirconia jar in a glovebox that was vigorously purged with nitrogen. The jar was then sealed for the ball milling process. Samples were also prepared in the same way with 0.025, 2.5, and 10% Sm. The 2.5 and 10% samples appear beige-yellow and dark mustard yellow, respectively; in particular the 10% sample is strongly colored, directly indicating the presence of a high Sm^{2+} concentration (see Figure S1 in the Supporting Information, SI).

For comparison, BaFCl doped with 2.5% and 10% Sm^{3+} (employing $SmCl_3{\cdot}6H_2O$ and SmF_3) were also prepared by ball milling. These samples are basically white (see Figure S1).

All peaks in the powder X-ray diffraction pattern of a 0.25% Sm^{2+} doped nanocrystalline BaFCl sample could be indexed to the BaFCl tetragonal matlockite structure with the space group of *P*4/*nmm* (see Figure S2 in the SI). From a Williamson-Hall analysis[22] of the prominent peaks and using Gaussian line shapes and eq 1, it follows that the crystalline size is around 30 nm with a microstrain parameter of about 0.06%.

$$B^2 \cos^2(\theta) = \left(\frac{\lambda}{D}\right)^2 + 16\varepsilon^2 \sin^2(\theta) \quad (1)$$

Received: March 26, 2014
Published: August 12, 2014

 © 2014 American Chemical Society dx.doi.org/10.1021/ic500712b | *Inorg. Chem.* 2014, 53, 8839−8841

In eq 1, B is the full width at half-maximum corrected for the instrumental width, λ is the wavelength of the X-ray (0.154 nm), and ε is the microstrain parameter. Interestingly, the unit cell lengths of the 10% sample are ∼1% larger compared with the samples with low dopant concentrations (see Figure S3 in the SI). For example, c increases from 7.19 to 7.26 Å because of the significant concentration of iodide (SmI_2 is used as the dopant) with a substantially larger ionic radius. This is in accord with the extensive studies by Kubel et al.[23]

Figure 1 displays the room temperature photoluminescence and excitation spectra of nanocrystalline BaFCl:Sm^{2+} (0.25%)

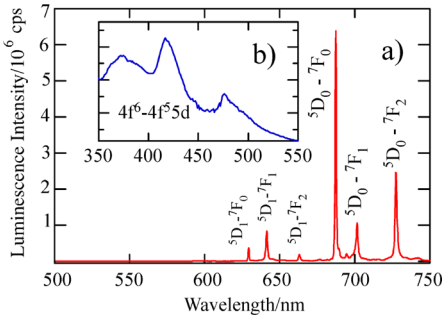

Figure 1. Room temperature emission (a) and excitation (b) spectra of BaFCl:Sm^{2+} (0.25%) as prepared by ball milling. The emission spectrum was excited at 415 nm (4 nm bandwidth); for the excitation spectrum, the emission at 687 nm was monitored. Major Sm^{2+} ^5D_J–^7F_J transitions are denoted.

prepared by ball milling. The photoluminescence spectrum consists mainly of narrow peaks at 628, 640, 662, 686, 700, 726, and 729 nm, which can readily be assigned to the ^5D_J–^7F_J transitions of the Sm^{2+} ions.[24] The excitation spectrum in Figure 1b clearly shows the f–d transitions of Sm^{2+}. Compared to Sm^{2+}, the Sm^{3+} emission lines are very weak, indicating that a large fraction of the samarium is indeed divalent. However, the intensities of the Sm^{2+} and Sm^{3+} ions cannot be used directly to compare the concentrations of the two ions because the Sm^{2+} and Sm^{3+} ions are excited via a parity-allowed f–d and a much weaker parity-forbidden f–f transition centered at 417 and 401 nm, respectively.

In order to estimate the ratio of Sm^{2+}/Sm^{3+}, the spectrum of BaFCl:Sm^{2+} (2.5%) was compared with BaFCl:Sm^{3+} (2.5%) before and after irradiation by 6 kGy of 40 kV X-ray (Figure 2). Spectra were excited by a 405 nm LED which overlaps well with the 401 nm Sm^{3+} absorption line. The 6 kGy X-irradiation converts ∼50% of the Sm^{3+} to Sm^{2+} in the ball milled sample as can be estimated from the luminescence spectra. For this calculation, a correction for excitation energy transfer (EET) from Sm^{3+} to Sm^{2+} ions has to be taken into account. The excited state lifetime of Sm^{3+} in the BaFCl:Sm^{3+} (2.5%) sample is 2.15 and 1.88 ms, for the nonirradiated and X-irradiated sample, respectively (see Figure S4 in the SI). Thus, EET occurs with a transfer rate of ∼70 s^{-1} and is not a major contributor (∼12%) to deactivation. From the Sm^{3+} intensities (e.g., $^4G_{5/2} \rightarrow {}^6H_{7/2}$), we conclude that >90% of the samarium ions are in the 2+ oxidation state.

The quantum efficiency for the Sm^{2+} luminescence in the BaFCl:Sm^{2+} samples prepared by ball milling is lower than for the X-ray induced Sm^{2+} emission in BaFCl:Sm^{3+} prepared by coprecipitation. For example, the 0.25% sample displays a luminescence intensity that is lower by a factor of ∼2. This is most likely caused by the 10-times smaller particle size of the

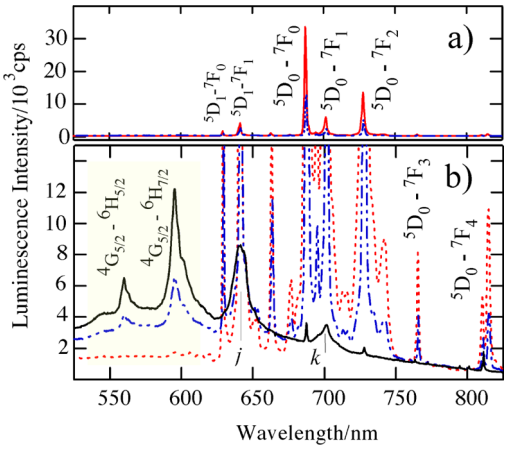

Figure 2. (a) Luminescence of BaFCl:Sm^{3+} (2.5%) after X-irradiation by 6 kGy (dashed line) compared to BaFCl:Sm^{2+} (2.5%; solid line; CCD acquisition time 0.5 s). (b) Close-up of Sm^{3+} transitions (CCD acquisition time 10 s). Nonirradiated and X-irradiated BaFCl:Sm^{3+} are shown as solid and dash-dot lines; the dotted line is for BaFCl:Sm^{2+} (2.5%). j and k indicate the $^4G_{5/2} \rightarrow {}^6H_{9/2}$, $^6H_{11/2}$ transitions.

ball-milled samples with a much higher surface defect density. Also, the BaFCl(I):Sm^{2+} (10%) sample prepared by ball milling (using SmI_2) displays a complex line shape (see Figure S5 in the SI) at low temperatures for the $^5D_0 \rightarrow {}^7F_0$ transition due to the variation in coordination for the Sm^{2+} ion.[25]

$$F(R) = \frac{(1-R)^2}{2R} \propto \frac{\varepsilon c}{s} \qquad (2)$$

Diffuse reflectance spectra of BaFCl:Sm^{3+} and BaFCl:Sm^{2+} (10%) are shown in Figure 3. The Sm^{3+} sample displays a f–f

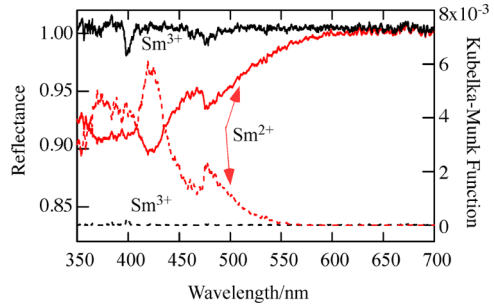

Figure 3. Diffuse reflectance spectra of BaFCl:Sm^{3+} (10%) and BaFCl(I):Sm^{2+} (10%) prepared by ball milling. Samples were mixed into $BaSO_4$ (280 and 87 mg in 2.6 g of $BaSO_4$ for BaFCl:Sm^{3+} and BaFCl(I):Sm^{2+}, respectively).

transition at 401 nm; this transition has a molar extinction coefficient of 3.3 in an aqueous solution of $SmCl_3 \cdot 6H_2O$. The Sm^{2+} sample exhibits the strong $4f^6 \rightarrow 4f^55d$ transitions centered around 417 nm, and by applying the Kubelka–Munk function[26] as given in eq 2 and using reflectance standards, we calculate a molar extinction coefficient ε of 400 (±50) M^{-1} cm^{-1} for this transition, yielding an overall oscillator strength $f \approx 10^{-3}$ for the $4f^6 \rightarrow 4f^55d$ transitions at 417 nm, in agreement with expectations.

Recently, the absorption coefficients for 0.5% Sm^{2+} doped $La_{0.125}Ba_{0.87}Cl_{2.13}$:$Sm^{2+}$ were reported.[27] The maximum of 80 cm^{-1} in the $4f^6 \rightarrow 4f^55d$ region corresponds to a molar extinction coefficient of 390 M^{-1} cm^{-1}, in excellent agreement

dx.doi.org/10.1021/ic500712b | Inorg. Chem. 2014, 53, 8839–8841

with the present result. Hence, we can safely conclude that most of the samarium is in the 2+ oxidation state. To determine the distribution of valence states, X-ray photoelectron spectroscopy has been applied to Eu^{2+}/Eu^{3+}.[28] However, for the present system, a shift of only 0.6 eV is observed for the 3d transition between Sm^{3+} and Sm^{2+} (Figures S7 and S8). The XPS results are further discussed in the SI.

The cathodoluminescence (CL) spectra shown in Figure 4 illustrate that the electron beam oxidizes some of the Sm^{2+} ions

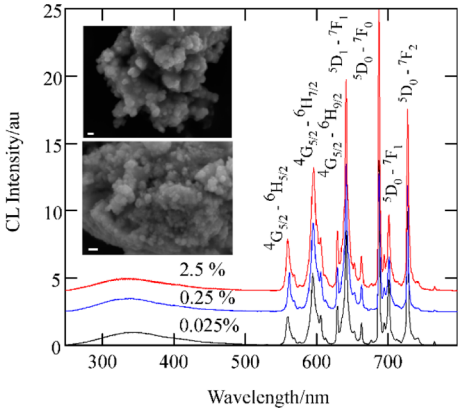

Figure 4. CL spectra of $BaFCl:Sm^{2+}$ (normalized at ~340 nm). Prominent Sm^{3+} ($^4G_{5/2}$-$^6H_{J/2}$) and Sm^{2+} (^5D_J-^7F_J) transitions are denoted. The inset shows SEM micrographs of the 0.25% (upper image; scale bar = 100 nm) and the 0.025% samples (lower image; scale bar = 200 nm).

to Sm^{3+}. In comparison with previously measured nanocrystals obtained by coprecipitation (average size of 300 nm), the 30 nm ball milled samples show an increased luminescence from Sm^{3+} in the CL measurement. This again is most likely caused by the much higher surface to volume ratio. The inserts in Figure 4 shows some typical SEM secondary electron images; the samples display irregularly shaped and aggregated particles. The average crystallite size is estimated to be 20 to 30 nm, in accord with the XRD result.

We have also investigated the stability of the Sm^{2+} in air; reflectance spectroscopy indicates no change over a time period of 2 days (see Figure S6 in the SI); i.e., the 2+ oxidation state is relatively stable. Naturally, it is likely that some of the Sm^{2+} close to the surface of the nanoparticles gets oxidized. We have also observed that intense blue light (420 nm) can photoionize Sm^{2+} in accord with previous findings.

Mechanochemical methods have a significant potential for the preparation of optical and X-ray storage phosphors, e.g., for the conventional $BaFBr:Eu^{2+}$ phosphor or any alkaline earth halide system in general. Diffuse reflectance and luminescence experiments are ideal for the investigation of the oxidation states of samarium in nanocrystalline materials.

■ ASSOCIATED CONTENT

Supporting Information

Experimental details, XRD patterns, XPS data, spectra, and lifetime measurements. This material is available free of charge via the Internet at http://pubs.acs.org.

■ AUTHOR INFORMATION

Corresponding Author

*Tel.: +61 (0)2 6268 8679. E-mail: h.riesen@adfa.edu.au.

Notes

The authors declare no competing financial interests.

■ ACKNOWLEDGMENTS

The Australian Research Council is acknowledged for financial support (ARC LP110100451). We thank Dr. Bill Bin Gong for conducting XPS experiments and Kate Badek for photographs of the samples. The Australian Microscopy & Microanalysis Research Facility at UNSW is acknowledged.

■ REFERENCES

(1) Fujita, K.; Yasumoto, C.; Hirao, K. *J. Lumin.* **2002**, *98*, 317−323.
(2) Mikhail, P.; Hulliger, J.; Schnieper, M.; Bill, H. *J. Mater. Chem.* **2000**, *10*, 987−991.
(3) Zeng, Q.; Kilah, N.; Riley, M.; Riesen, H. *J. Lumin.* **2003**, *104*, 65−76.
(4) Winnacker, A.; Shelby, R. M.; Macfarlane, R. M. *Opt. Lett.* **1985**, *10*, 350−352.
(5) Nogami, M.; Suzuki, K. *J. Phys. Chem. B* **2002**, *106*, 5395−5399.
(6) Wang, J.; Huang, Y.; Li, Y.; Seo, H. J. *J. Am. Ceram. Soc.* **2011**, *94*, 1454−1459.
(7) Qiu, J.; Miura, K.; Suzuki, T.; Mitsuyu, T.; Hirao, K. *Appl. Phys. Lett.* **1999**, *74*, 10−12.
(8) Liu, Z.; Stevens-Kalceff, M. A.; Riesen, H. *J. Phys. Chem. A* **2013**, *117*, 1930−1934.
(9) Pei, Z.; Su, Q.; Zhang, J. *J. Alloys Compd.* **1993**, *198*, 51−53.
(10) Nogami, M.; Suzuki, K. *Adv. Mater.* **2002**, *14*, 923−926.
(11) Malchukova, E.; Boizot, B.; Ghaleb, D.; Petite, G. *Nucl. Instrum. Methods Phys. Res., Sect. A* **2005**, *537*, 411−414.
(12) Malchukova, E.; Boizot, B.; Petite, G.; Ghaleb, D. *J. Non-Cryst. Solids* **2007**, *353*, 2397−2402.
(13) Park, G. J.; Hayakawa, T.; Nogami, M. *J. Phys.: Condens. Mater.* **2003**, *15*, 1259−1265.
(14) Riesen, H.; Kaczmarek, W. A. *International PCT Application*, WO 2006063409-A1, 2005.
(15) Riesen, H.; Kaczmarek, W. A. *Inorg. Chem.* **2007**, *46*, 7235−7237.
(16) Liu, Z.; Stevens-Kalceff, M. A.; Riesen, H. *J. Phys. Chem. C* **2012**, *116*, 8322−8331.
(17) Stevens-Kalceff, M. A.; Liu, Z.; Riesen, H. *Microsc. Microanal.* **2012**, *18*, 1229−1238.
(18) Vanysek, Petr. Electrochemical Series. In *Handbook of Chemistry and Physics*, 87th ed.; Chemical Rubber Company: Boca Raton, FL, 2006.
(19) Wang, X.; Liu, Z.; Stevens-Kalceff, M. A.; Riesen, H. *Mater. Res. Bull.* **2013**, *48*, 3691−3694.
(20) Glushenkov, A.; Zhang, H.; Zou, J.; Lu, G.; Chen, Y. *Nanotechnology* **2007**, *18*, 175604−1−5.
(21) Liu, Z.; Stevens-Kalceff, M. A.; Wang, X.; Riesen, H. *Chem. Phys. Lett.* **2013**, *588*, 193−197.
(22) Williamson, G. K.; Hall, W. H. *Acta Metall.* **1953**, *1*, 22−31.
(23) Kubel, F.; Hagemann, H.; Bill, H. *Mater. Res. Bull.* **1995**, *30*, 405−412.
(24) Gacon, J. C.; Grenet, G.; Souillat, J. C.; Kibler, M. *J. Chem. Phys.* **1978**, *69*, 868−880.
(25) Jaaniso, R.; Hagemann, H.; Bill, H. *J. Chem. Phys.* **1994**, *101*, 10323−10337.
(26) Kortüm, G. *Reflectance Spectroscopy*; Springer-Verlag: New York, 1969.
(27) Dixie, L. C.; Edgar, A.; Reid, M. F. *J. Lumin.* **2012**, *132*, 2775−2782.
(28) He, J.; Wang, Y.; Liu, Y.; Wang, K.; Li, R.; Fan, J.; Xu, S.; Zhang, L. *J. Phys. Chem. C* **2013**, *117*, 21916−21922.